



# Comparisons Between Modeling and Measured Performance of the BNL Linac\*

D. Raparia, J. G. Alessi, A. Kponou  
Brookhaven National Laboratory  
Upton, NY, 11973, USA

## Abstract

Quite good agreement has been achieved between computer modeling and actual performance of the Brookhaven 200 MeV Linac. We will present comparisons between calculated and measured performance for beam transport through the RFQ, the 6 m transport from RFQ to the linac, and matching and transport through the linac.

## 1 INTRODUCTION

The Brookhaven 200 MeV linac serves as the injector for the AGS Booster and as well delivers beam to the Brookhaven Isotope Resource Center. It consists of a 35 keV magnetron surface plasma source, a low energy beam transport (LEBT) [1], 201 MHz radio frequency quadrupole (RFQ) [2], medium energy beam transport (MEBT) and 200 MeV Linac [3]. In this last year we have gone through a linac upgrade to get 2.5 more average current ( $146 \mu\text{A}$ ) [4]. This was achieved by increasing repetition rate 5 to 7.5 Hz and increasing peak current from 25 to 39 mA. In this paper we compare computer modeling with actual performance.

## 2 LEBT AND RFQ

LEBT had two pulsed solenoids, two sets of x and y steerer, beam chopper, emittance probe, and two current toroids. The chopper was removed from the line, making the line shorter by 70 cm. Computer modeling of this line showed that we should move the 1st solenoid as close to the ion source as possible to reduce the beam size in the 1st solenoid and the second solenoid as close to the RFQ as possible to increase the convergence angle required by the RFQ acceptance. Figure 1 shows the ion trajectories through this line and phase space at the exit of the ion source, middle of the line and entrance of RFQ. The RFQ acceptance is shown as a solid line ellipse. This calculation assumed that the beam space charge is neutralized.

Shortening of the line resulted in lower measured emittance. Due to lower emittance and better matching transmission through the RFQ was improved by about 10 percent. Figure 2 shows the transmission as a function of input beam current.

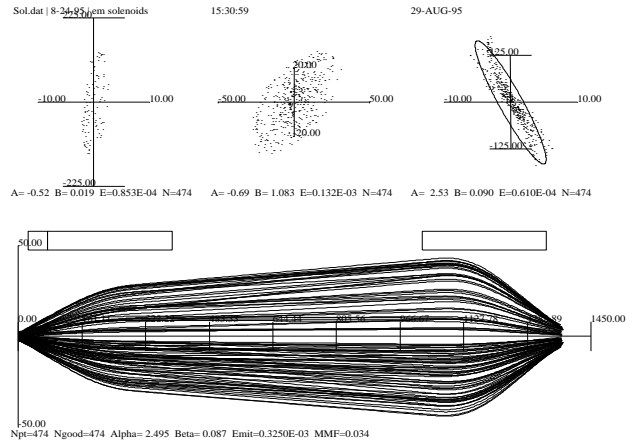


Figure 1: Ion trajectories through the LEBT and phase space at ion-source, middle of the line, and at the entrance of the RFQ.

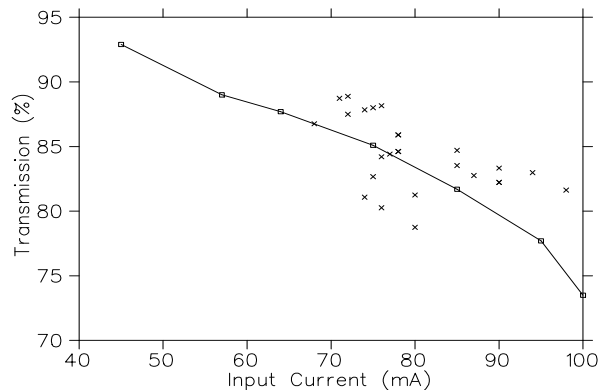


Figure 2: RFQ transmission as a function of input current. The solid line indicates the simulation and crosses the measured values.

\* Work performed under the auspices of the U. S. Department of Energy.

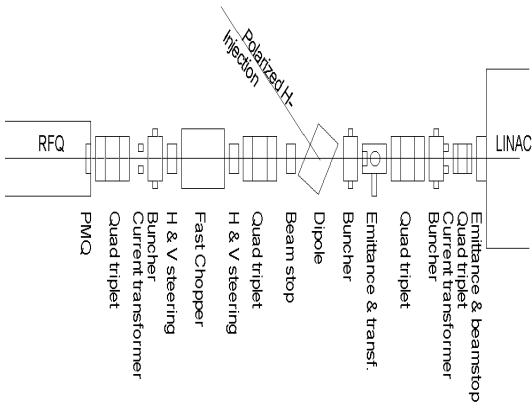


Figure 3: MEBT, 750 keV Transport Line.

### 3 MEBT AND LINAC

This is where we have recovered most of the beam losses. This line is 6 meter long and is shown in Figure 3. It consists of four triplets, three bunchers, one slow chopper, one fast chopper, two emittance measurement units, three current transformers, two sets of x, y steerers, and a dipole to accommodate polarized beam coming at 60 deg angle. The ideal match between RFQ and DTL could have been obtained with a  $5\beta\lambda$  long FODO lattice with quadrupole spacing about  $\beta\lambda$  and at least two bunchers. But the requirement of beam chopping and polarized beam dictated a triplet solution [5].

The first quadrupole after the RFQ was too far; by the time the beam reached the quadrupole it had gone through a waist in the x plane, hence was diverging in both planes. No matter which polarity quad one puts, beam size in the other direction is very big. Also the longitudinal beam size is too big before it reaches the first buncher. To improve the capture and transmission of the beam in MEBT, the RFQ end flange at the high energy end was modified to accommodate a permanent magnet quadrupole (PMQ). The PMQ was similar to one as used in the SSC DTL [6]. We have also rearranged the gate valve and current transformers at the beginning of the line, and also measured and aligned all the quadrupoles very carefully. Measurement as well as simulation showed that as little as a 1.5 degree quadrupole rotation can increase the emittance by 50 %. The last quadruplet was changed to a triplet to reduce coupling. Figure 4, shows the measured and calculated phase spaces after the second buncher. Table 1 shows calculated (TRACE3D) and measured Twiss parameters for Figure 4.

Table 2, compares measurements and PARMILA results at various locations. We believe that lower values for currents after the second buncher and at the entrance of the Linac are caused by the grids in the

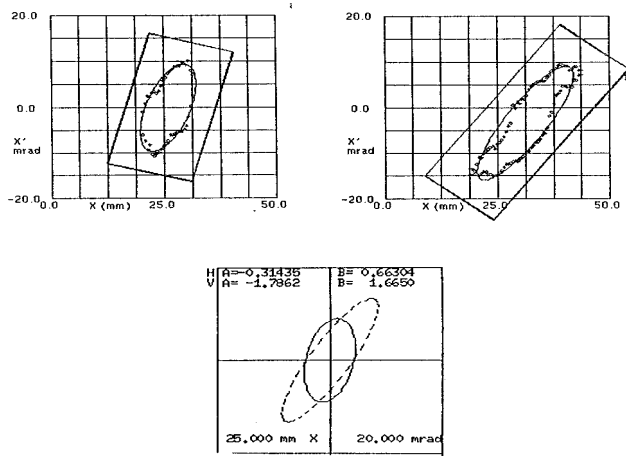


Figure 4: Measured (upper two) and calculated (lower) phase space after the second buncher.

Planes	X			Y		
	$\alpha_x$	$\beta_x$	$\epsilon_x$	$\alpha_y$	$\beta_y$	$\epsilon_y$
Meas.	-0.60	0.79	9.71	-1.59	1.61	13.82
Cal.	-0.31	0.66	9.80	-1.79	1.67	14.00

Table 1: Calculated and measured Twiss parameters after the second buncher.  $\beta$  is in mm/mrad and  $\epsilon$  (unnor.,RMS) in  $\pi$  mm mrad.

buncher drift tubes (four in each buncher). These grids are placed in the bunchers to reduce RF defocusing effects. Emittance measurements at 200 MeV are done using profiles at five places. Agreement between calculations and measured Twiss parameters at 200 MeV is poor because there are 295 quadrupoles, and calibration and misalignment errors are not known to a good accuracy.

Location	94-95		95-96	
	Sim.	Meas.	Sim.	Meas.
Current mA				
RFQ	50.0	50.0	62.9	62.9
Buncher	50.0	41.0	62.9	57.8
MEBT	42.4	37.3	62.9	53.2
Tank 1	27.4	28.4	37.1	37.7
Tank 9	26.2	26.7	36.4	35.9
Emittance, (nor,RMS) $\pi$ mm mrad				
RFQ	0.400	0.400	0.375	0.375
Buncher	0.44	0.56	0.47	0.57
200 MeV	1.32	2.8	1.85	1.92

Table 2: Comparison between simulations and measured beam parameters.

## 4 ALGEBRAIC RECONSTRUCTION TECHNIQUE (ART)

A radiograph of the beam at the BLIP target taken last year showed a tilted ellipse in the x-y plane. Sources of this coupling can be quad rotation or vertical offset in the dipole. This triggered the need for an x-y density profile. We found that algebraic reconstruction technique (ART) could help us. ART was introduced by Gordan, Bender and Herman [7] for solving the problem of three dimensional reconstruction from projections. The ART algorithms have a simple intuitive basis. Each projected density is thrown back across the reconstruction space in which the densities are iteratively modified to bring each reconstructed projection into agreement with the measured projection. The reconstruction space is an  $n \times n$  array of small pixels,  $\rho$  is grayness or density number which is uniform within the pixel but different from other pixels. Assume  $\mathbf{P}$  is a matrix of  $m \times n^2$  and the  $m$  component column vector  $\mathbf{R}$ . Let  $p_{i,j}$  denote the  $(i,j)$ th element of  $\mathbf{P}$ , and  $R_i$  denote the  $i$ th element of reconstructed projection vector  $\mathbf{R}$ . For  $1 \leq i \leq m$ ,  $N_i$  is number of pixels under projection  $R_i$ , defined as  $N_i = \sum_j p_{i,j}^2$ . The density number  $\rho_j^q$  denotes the value of  $\rho_j$  after  $q$  iterations.

After  $q$  iterations the intensity of the  $i$ th reconstructed projection ray is

$$R_i^q = \sum_j p_{i,j} \rho_j^q,$$

and the density in each pixel is

$$\rho_j^{\sim q+1} = \rho_j^q + p_{i,j} \frac{R_i - R_i^q}{N_i} \quad \text{with starting value } \rho_j^{\sim 0} = 0$$

where  $R_i$  is the measured projection and,

$$i = \begin{cases} m, & \text{if } (q+1) \text{ is divisible } m \\ \text{the remainder of dividing } (q+1) \text{ by } m, & \text{otherwise} \end{cases}$$

and,

$$\rho_j^q = \begin{cases} 0, & \text{if } \rho_j^{\sim q} \leq 0 \\ \rho_j^{\sim q}, & \text{if } 0 \leq \rho_j^{\sim q} \leq 1 \\ 1, & \text{if } \rho_j^{\sim q} \geq 1 \end{cases}$$

It is necessary to determine when an iterative algorithm has converged to a solution which is optimal according to some criterion. We are using as the criteria of convergence the discrepancy between the measured and calculated projection elements

$$D^q = \left\{ \frac{1}{m} \sum_{i=1}^m \frac{(R_i - R_i^q)^2}{N_i} \right\}^{\frac{1}{2}}$$

We have added a third wire at 45 degree in wire scanners in two places. Figure 5 compares the measured and reconstructed profiles in the BLIP transfer line [8] after the 1st octupole and figure 6 shows the reconstructed 3D density distribution.

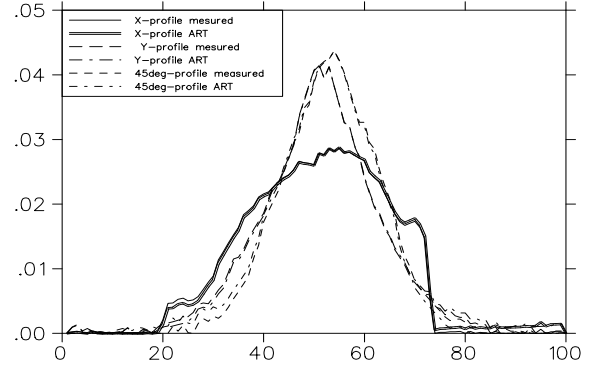


Figure 5: Beam projection on x, y, and 45 degree planes.

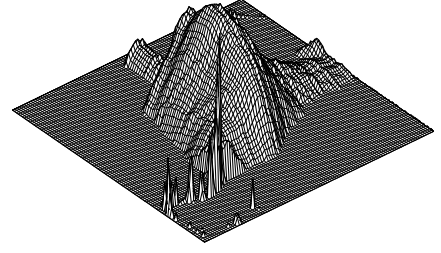


Figure 6: Reconstructed 3D density distribution using ART.

## 5 REFERENCES

- [1] J. G. Alessi, *et al*, "The AGS H<sup>-</sup> RFQ Preinjector" Proc. 1988 Linear Accelerator Conference, CEBAF-Report-89-001, pp196. (1989).
- [2] R. A. Gough, *et al*, "Design of an RFQ Based H<sup>-</sup> Injector for the BNL/FNL 200 MeV Proton Linacs", Proc. 1986 Linear Accelerator Conference, SLAC-Report-303, pp303 (1986).
- [3] G. W. Wheeler, *et al*, "The Brookhaven 200 MeV Proton Linear Accelerator", Particle Accelerator, Vol. 9, pp 1, (1979).
- [4] J. G. Alessi, *et al*, "Upgrade of the Brookhaven 200 MeV Linac", these Proceeding.
- [5] D. Raparia, "RFQ-DTL Matching Solution For Different Requirements" Proc. 1995 Particle Accelerator Conference, pp1385 (1995).
- [6] D. Raparia, *et al*, "SSC Drift-Tube Linac Design", Proc. 1992 Linear Accelerator Conference, AECL-10728, Vol1, pp199 (1992).
- [7] R. Gordon, *et al*, "Three-Dimensional Reconstruction from Projections: A Review of Algorithms", International Review of Cytology, Vol. 38, pp 111, (1974).
- [8] A. Kponou, *et al*, these proceeding.